Molecular Genetics and Genomics (2020) 295:1103–1111
https://doi.org/10.1007/s00438-020-01686-6

ORIGINAL ARTICLE

A hemizygous mutation in the androgen receptor gene causes different phenotypes of androgen insensitivity syndrome in two siblings by disrupting the nuclear translocation

Chunjie Liu[1] · Yongfen Lyu[1] · Pin Li[1]

Received: 11 November 2019 / Accepted: 6 May 2020 / Published online: 20 May 2020

Abstract

The androgen insensitivity syndrome (AIS) is a congenital disease characterized by androgen resistance due to androgen receptor (*AR*) gene mutations, resulting in disorders of sex differentiation in 46,XY individuals. However, the underlying mechanisms in the majority of *AR* variants and the phenotype–genotype correlations are unclear. Here, we identified a p.Y764H variant of the *AR* gene that results in different phenotypes in a family. Structural analyses revealed that amino acid substitution affected protein properties and spatial conformation, and in vitro, functional studies showed impaired nuclear translocation ability of the mutated protein. Moreover, the extent to which this variant reduced nuclear translocation depends on the dihydrotestosterone (DHT) concentrations. Our results, for the first time, demonstrated a pathogenesis of the p.Y764H mutations in *AR* resulting in AIS phenotype, and indicated that AIS patients with p.Y764H mutation and preserved gonad might have residual AR activity at high androgen levels, putting patients at risk for pubertal virilization in the future. We provide an in-depth insight into the pathogenesis in AIS based on the amino acid substitution, which may help aid its precise diagnosis, personalized treatment, and organized follow-up to avoid gender dysphoria.

Keywords Androgen insensitivity syndrome · Androgen receptor gene · Variants · Pubertal virilization

Introduction

The androgen insensitivity syndrome (AIS) (MIM: 300068) is a congenital X-linked recessive disease resulting in disorders of sex differentiation, caused by complete or partial resistance to androgens in 46, XY karyotype individuals (Batista and Costa 2018). According to the degree of feminization of the external genitalia, the clinical phenotypes can be divided into three categories: complete androgen insensitivity syndrome (CAIS), partial androgen insensitivity syndrome (PAIS), and mild androgen insensitivity syndrome (MAIS) (Hughes et al. 2012; Vaidyanathan and Kaplowitz 2018). The estimated prevalence of CAIS ranges from 1:20,400 to 1:99,100 in 46, XY males (Boehmer and Brinkmann 2001; Hughes et al. 2012). AIS adversely affects the physical and mental health of children, especially for patients with CAIS or PAIS who are raised as females. Improper diagnosis or management will increase the risk of testicular tumor occurrence and potential pubertal virilization, which might induce gender dysphoria. An in-depth analysis of AIS pathogenesis is essential for further clinical treatment of the disease.

Researchers have made significant progress in enhancing the understanding of the molecular causes of AIS during sexual development. A pathogenic mutation of the androgen receptor gene (*AR*; MIM: 313,700), which leads to abnormal protein structure, has been established as an important cause of androgen resistance. The *AR* gene is located on Xq11–12 and is more than 90-kb length, contains 8-exons, and encodes a protein with 920 amino acid residues. The AR protein consists of four major functional domains: the N-terminal domain (NTD), the DNA-binding domain (DBD), the C-terminal

Communicated by S. Hohmann.

Electronic supplementary material The online version of this article (https://doi.org/10.1007/s00438-020-01686-6) contains supplementary material, which is available to authorized users.

✉ Pin Li
lipin2019@126.com

[1] Department of Endocrinology, Shanghai Children's Hospital, Shanghai Jiao Tong University, Shanghai 200062, People's Republic of China

ligand-binding domain (LBD), and a hinge region that connects the LBD to DBD (Wang and Lu 2001; Jaaskelainen 2012; Chauhan and Rani 2018). The AR protein, a steroid-activated transcription factor, is necessary for normal prenatal male sexual development and pubertal development of the sexual characteristics. After activation of AR by the androgens (testosterone, T or dihydrotestosterone, DHT), the protein dissociates from the heat shock proteins (Hsps) and translocates from the cytoplasm to the nucleus. In the nucleus, the protein binds to the androgen response element on the target genes and subsequently regulates androgen-responsive gene expression at the transcriptional level (Sakkiah and Ng 2016; Yuan and Zhang 2018). To date, about 600 variants in the *AR* gene have been recorded in HGMD (https://www.hgmd.cf.ac.uk/). Among these, the most common variants are point mutations (Gottlieb and Beitel 2012; Infante and Alvelos 2016; Chauhan and Rani 2018). In CAIS and PAIS, missense mutations are mainly distributed in exons encoding the LBD or DBD, leading to significant impairment in cell response to androgens or DNA binding (Matias and Donner 2000; Hughes et al. 2012). According to the *AR* mutation database (https://androgendb.mcgill.ca/), some individuals may have different phenotypes with the same mutation (Gottlieb and Beitel 2012). Hitherto, the correlation between phenotype and genotype in AIS is still unclear.

Clinically, the time of gonadectomy in patients with CAIS who were raised as females is generally delayed to allow spontaneous puberty and permit patients to make informed choices. In PAIS patients with predominantly female genitalia, prepubertal gonadectomy helps to avoid the emotional discomfort of increasing clitoromegaly at the time of puberty. However, in some PAIS patients raised as females and conserved gonads, the risk of potential pubertal virilization should be noted. Thus, in vitro studies of *AR* mutations are essential to help understand the pathogenic mechanisms and potential pubertal virilization due to the residual AR activity. In this study, we reported a family in which the proband and her brother had CAIS and PAIS, respectively. Interestingly, whole-exome sequencing identified the same nonsynonymous hemizygous mutation of p.Y764H in the LBD of the *AR* gene in both the siblings. We further performed in vitro structural and functional studies, to investigate the pathogenesis of the mutation resulting in AIS phenotypes and better predict the future pubertal sexual function based on the mutation.

Methods

Patients and samples

Our study recruited a Chinese family, in which the proband and her brother were clinically suspected to have CAIS and PAIS, respectively. The proband exhibited CAIS and was raised as a girl, while the elder brother raised as a boy was suspected of having PAIS. Both parents were healthy (Fig. 1a). The ethics committee of Shanghai Children's Hospital approved this study, and all participants gave informed consent for their participation.

The proband (II-4), a 3-month-old girl, was first referred to Shanghai Children's Hospital due to a right inguinal hernia. Physical examination showed normal female external genitalia. Karyotype analysis confirmed 46, XY; and FISH analysis showed that the SRY gene was positive. Ultrasonography revealed the absence of a uterus and ovaries; the presence of a testis sized $15 \times 7 \times 8$ mm located below the right hernia sac, and a testis-like structure sized $15 \times 6 \times 7$ mm at the left inguinal canal that was considered the left testis. The concentrations of serum hormones were as follows: *T*, 1.34 nmol/L (norm level for boys this age [nl]: < 0.69 nmol/L); luteinizing hormone (LH), 0.55 IU/L (nl: < 0.2 IU/L); and follicle-stimulating hormone (FSH), 0.89 IU/L (nl: 0.19–2.7 IU/L). At 15 months of age, the GnRH stimulation test and HCG stimulation test were performed. The peak stimulated levels of LH and FSH were 28.77 IU/L and 3.03 IU/L, respectively. The HCG stimulation test showed that the T level increased from 2.43 to 7.52 nmol/L, and DHT value increased from 12.16 to 44.50 pg/ml. Topical dihydrotestosterone gel was applied for 2 months, and the clitoris was not enlarged. Thus, the diagnosis of CAIS was considered.

The elder brother (II-3) had a micropenis, perineal hypospadias, a bifid scrotum, and penoscrotal transposition at birth. The karyotype was 46, XY, and the SRY gene analysis was positive. The GnRH stimulation test showed that stimulated peak levels of LH and FSH were 48.2 IU/L and 2.22 IU/L, respectively. At 19 months of age, he underwent urethroplasty for hypospadias, penile straightening, and correction of penoscrotal transposition. At 4 years of age, the HCG stimulation test showed that the T level increased from < 0.35 to 10.24 nmol/L, and DHT level increased from 9.0 to 180.49 pg/ml. Currently, the patient is being raised as a boy and combined with the medical history, the diagnosis of PAIS was discussed.

Whole-exome sequencing analysis and mutation screening

Peripheral blood samples were obtained from the proband and other family members, and DNA was extracted using the QIAamp DNA Blood Midi Kit (Qiagen, Duesseldorf, Germany) following the manufacturer's instructions. We performed whole-exome sequencing of the patients (II-3 and II-4). The DNA was sequenced using the Illumina HiSeq X10 platform at a commercial provider (Shanghai Fulgent Genetics Biotechnology Co., Ltd, Shanghai, China). The

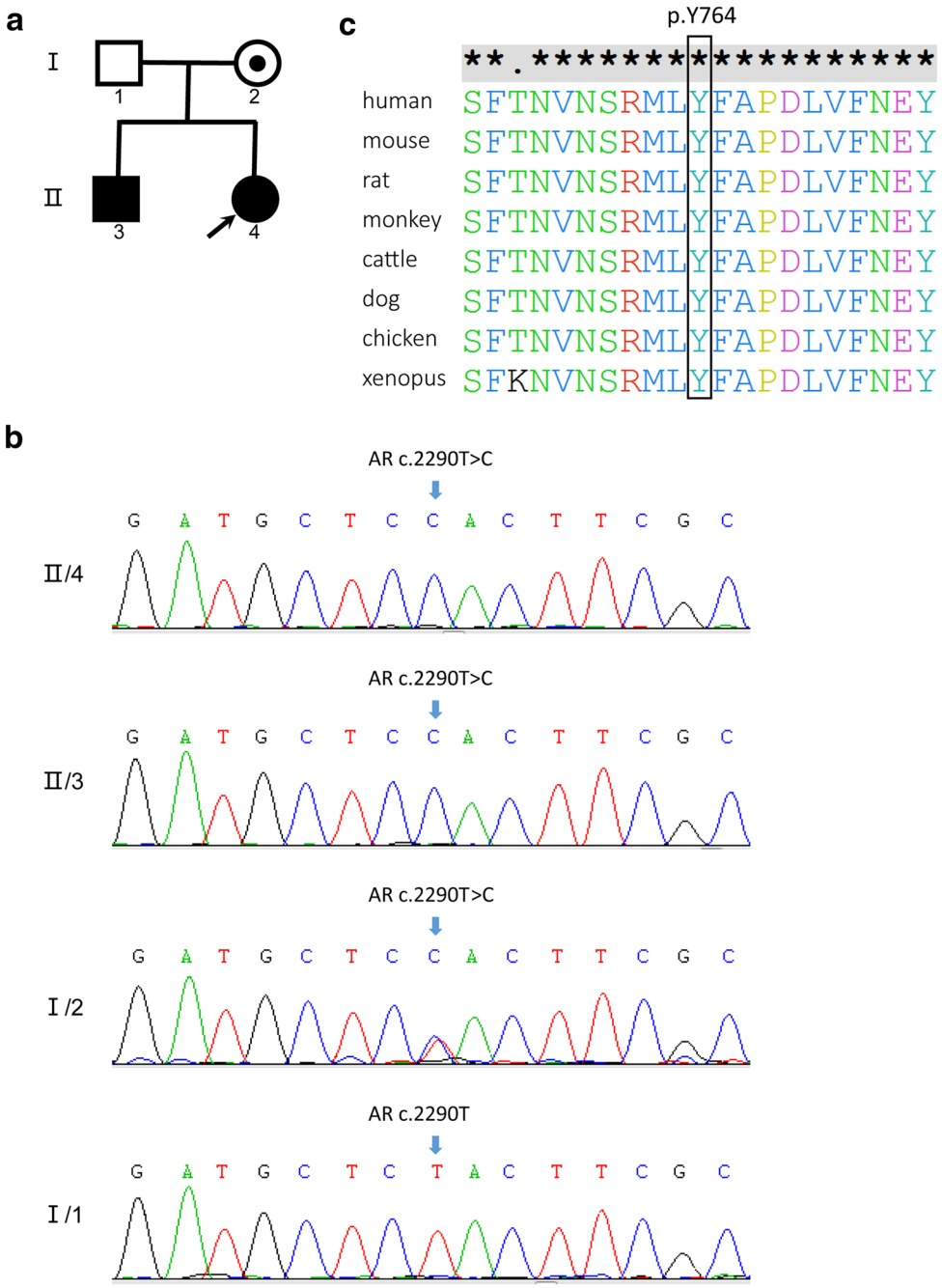

Fig. 1 A hemizygous mutation (c.2290T > C, p.Y764H) in the *AR* gene identified in a family with different phenotypes. **a** Pedigree of the family. The proband (II-4) is indicated by an arrow who exhibited CAIS. Her brother (II-3) had PAIS. Black symbols: affected individuals; open symbols: unaffected individuals; black spots: carriers. **b** Gene sequencing peaks of the mutation in the *AR* gene in the patients and their relatives. Arrows indicate the location of the mutation sites. DNA sequencing in the proband (II-4) and her brother (II-3) showed a nonsynonymous T to C transition at nucleotide 2290 in the hemizygous form, resulting in tyrosine to histidine mutation at codon 764. The mother (I-2) of the proband was a heterozygous carrier for the mutation. The proband's father (I-1) was unaffected at this site. **c** Alignment of the amino acid sequences of AR orthologues among several different species. The region of AR protein with the amino acid residue Y764 is highly conserved across the species

quality of the data was good enough to confirm the mutation (Tables S1 and S2).

Filtering criteria were set as follows: (1) variants located in exonic or splicing region, (2) functional mutations defined as nonsynonymous single nucleotide variants (SNVs), stop-gain mutations, stop-loss mutations, frameshift or non-frameshift deletions or insertions, and splice-site mutations, excluding synonymous variants, (3) frequency lower than 0.1% according to public variant databases 1000 Genomes and Exome Aggregation Consortium (ExAC), and (4) at least one scoring software analysis suggesting that mutation is deleterious. Next, we used PubMed to search for the candidate genes that had been related to AIS. Candidate mutations were confirmed by Sanger sequencing in the family members.

Bioinformatics study and homology analysis

The Mutation Taster (www.mutationtaster.org), polymorphism phenotyping-2 (PolyPhen-2, https://genetics.bwh.harvard.edu/pph2/), and Sorting Intolerant from Tolerant

(SIFT, https://sift.bii.a-star.edu.sg/) programs were used to predict the disease-causing potential of a variant.

For homology analysis, protein sequences of various species of AR were obtained from NCBI (https://www.ncbi.nlm.nih.gov/) and blasted by ClustalX2 software.

Three-dimensional reconstruction of AR mutant protein

Alterations of protein properties and structures were analyzed by HOPE (www.cmbi.ru.nl/hope). SWISS PDB viewer was used for the analysis of the spatial conformation of both the wild-type and the mutant residues of AR.

Plasmid construction and site-directed mutagenesis

Human full-length *AR* cDNA (*AR*, NM_000044.6) was amplified from the AR expression plasmid (pHBLV000461-*AR*) purchased from a commercial provider (Hanbio Biotechnology Co., Ltd, Shanghai, China). The primers used for PCR are listed as follows:

F: 5′-AGAGGATCTATTTCCGGTGAATTCGCCACC ATGGAAGTGCAGTTAGGGC -3′

R: 5′-CACTTAAGCTTGGTACCGAGGATCCCTGGG TGTGGAAATAGATGGGCTT -3′

Amplicons were inserted into the PC013-pcDNA3.1-CMV-MCS-3FLAG-EF1-ZsGreen-T2A-PURO vector (Hanbio Biotechnology Co., Ltd) at the site of EcoR1 and BamH1 using the HB-infusion™ Master mix, yielding the fusion protein expression plasmid *AR*-WT (WT, wild type).

The mutant *AR* cDNA was constructed using pHBLV000461-*AR* as a template, and the KOD-Plus PCR kit (TOYOBO, Osaka, Japan) was used to introduce the mutant site with mutated primers:

F: 5′-CTACTAGAGGATCTATTTCCGGTGAATTCG CCACCATGGAAGTGCAGTT-3′

r: 5′- AGATCAGGGGCGAAGTGGAGCATCCTGGAG -3′

f: 5′- CTCCAGGATGCTCCACTTCGCCCCTGATCT-3′

R: 5′-R:CACTTAAGCTTGGTACCGAGGATCCCT GGGTGTGGAAATAGATGGGCTT -3′.

The mutant amplicons were subcloned into PC013-pcDNA3.1-CMV-MCS-3FLAG-EF1-ZsGreen-T2A-PURO vector as well, forming the mutant plasmid *AR*-Y764H.

Both wild-type and mutant *AR* plasmids were sequenced to confirm the desired fragments. For transient transfection, the plasmids were prepared using the Qiagen Plasmid Midi kit (Qiagen, Germany).

Cell culture and transfection

Monkey kidney COS-7 cells were maintained at 37 ℃ under a humidified atmosphere with 5% CO_2 in DMEM high glucose medium (no Phenol Red) (Gibco, USA) with 10% fetal bovine serum (Gibco, USA), and penicillin–streptomycin (Gibco, USA).

For determining the nuclear localization, COS-7 cells were seeded in 24-well plates on glass coverslips (0.48×10^5 cells in 0.5 mL). Upon reaching 70–80% confluence, COS-7 cells were transfected with 500-ng *AR*-WT plasmid, 500-ng *AR*-Y764H plasmid, or 500-ng negative control (NC) plasmid (empty vector) using Lipofectamine 2000 reagent (Invitrogen, USA) following the manufacturer's protocol. Reduced serum medium—Opti-MEM (no phenol red, Gibco, USA) was used for the preparation of DNA-lipid complexes.

Immunofluorescence and subcellular localization

Twenty-four hours after transfection, cells were treated with 0.1-, 1-, 10-, or 100-nM DHT (B8214, Apex BIO, USA) or DMSO, respectively. Four hours after hormone stimulation, the cells were washed twice with phosphate-buffered saline (PBS), then fixed for 30 min at room temperature with 4% paraformaldehyde made fresh in 1X PBS, soaked twice for 20 min each in absolute ethanol, washed once with PBS, permeabilized twice for 10 min each time with 0.1% Triton X-100/0.2% BSA in PBS, and blocked for 1 h at room temperature with PBS containing 1% BSA, 4% normal serum, and 0.4% Triton X-100. The cells were incubated overnight with a 1:200 dilution of a mouse anti-DDDDK-Tag mAb (AE005, ABclonal, China). After washing three times with PBT (0.1% Triton X-100 in 1XPBS) for 10 min each time, cells were incubated with $Cy^{TM}3$ AffiniPure Goat Anti-Mouse lgG (H + L) (Jackson, USA), a secondary antibody at a dilution of 1:100 for 1-h shielding from light. The cells were washed with PBT three times for 10 min each, the cell nuclei stained with 4, 6-diamidino-2-phenyl indole (DAPI, C1005, Beyotime, China), and cells washed twice with PBS. Coverslips were mounted in Fluoromount-G (SouthernBiotech, America), and the cells were observed and photographed with an Olympus Fluoview 1000 laser confocal microscope (Olympus, Japan) with a 20 × objective lenses (Olympus). The immunofluorescence quantitative analysis was performed using the Image J software. Mann–Whitney *U* tests or unpaired Student's *t* tests were used for statistical analysis.

Results

Identification of a rare candidate variant in the *AR* gene

To explore the molecular causes of patients with AIS, we performed whole-exome sequencing to identify possible pathogenic variants of the patients. We screened the

sequencing data for rare mutations. According to the filtering criteria which were described in the methods section, finally, a rare nonsynonymous hemizygous mutation (c.2290T > C, p.Y764H) in exon 5 of the *AR* gene was detected in both the proband and her brother. There were no other pathogenic mutations identified in the *AR* gene and common known 46,XY DSD-related genes, including *SRY, SOX9, NR5A1/SF1, WT1, GATA4, ZFPM2, CBX2, MAP3K1, DMRT1, DHH, MAMLD1, DAX1, SRD5A2, HSD17B3, STAR, CYP17A1, AMHR, LHCGR* (Bashamboo and McElreavey 2016; Nagaraja and Gubbala 2019) in the two siblings.

Gene sequencing peaks confirmed the same hemizygous mutation of p.Y764H in the proband (II-4, CAIS) and her elder brother (II-3, PAIS), and heterozygous mutation in their mother (I-2). The father (I-1) of the proband was normal at this site, thus suggesting that the patients inherited the variant gene from their mother (Fig. 1b).

Bioinformatic and homology analysis of the *AR* variant

We used online software to predict the pathogenicity of the mutant protein. SIFT, Polyphen-2, and Mutation Taster predicted the mutant protein to be deleterious, probably damaging, and disease-causing, respectively, thus confirming our result that *AR*-p.Y764H has high potential to cause disease.

Moreover, multiple amino acid sequence alignments of AR orthologues revealed highly conserved Y764 residue across the species, suggesting preservation of this amino acid through evolution, which might play an essential role in maintaining protein function (Fig. 1c).

3D protein structure analysis of the mutant protein

Next, we analyzed the impact of *AR* mutation on amino acid properties and domain functions by HOPE online software (Venselaar and Beek 2010). The mutation of tyrosine to histidine at position 764 introduces an amino acid with different properties. The mutant residue is smaller than the wild-type residue. The mutation leads to a space in the core of the protein and loss of hydrophobic interactions. The mutated residue is not in direct contact with the ligand. However, the mutation could affect the local stability and subsequently impact the ligand contacts made by one of the neighboring residues (Venselaar and Beek 2010) (Fig. 2a, b).

To further predict the functional changes of the mutation, the spatial conformation of both the wild-type and mutant residues was constructed using the SWISS PDB viewer. Typically, Y764 (TYR764) interacts with ARG753 with two hydrogen bonds and with SER754 with one hydrogen bond. When tyrosine (TYR, Y) at position 764 is mutated to histidine (HIS, H), the hydrogen bonds in the three-dimensional structure and spatial conformation of AR protein were altered. Mutated residue HIS764 still interacts with ARG753 and SER754 with hydrogen bonds. In addition, another hydrogen bond forms with asparagine at position 757 (ASN757, located in helix 5) (Fig. 2c, d).

Subcellular localization of AR in COS-7 cells

To further investigate whether the p.Y764H mutation of the AR protein could influence its nuclear translocation, we evaluated the subcellular localization of this mutant protein in the COS-7 cell line. Cells were transfected with the NC plasmid, *AR*-WT, or *AR*-Y764H plasmid. Following DHT treatment at different concentrations (0.1-, 1-, 10-, or 100-nM DHT), the localization of wild-type and the mutant fusions were analyzed by immunofluorescence staining. Transfection of the NC plasmid showed no red fluorescent signals in either the cytoplasm or nucleus (Fig. 3a, d, g, j, m). Treated with DMSO, as the control, both the wild-type and mutant proteins localized to the cytoplasm (Fig. 3b, c). After treatment with 0.1-nM DHT, 51.94% of AR-WT protein translocated from cytoplasm to nucleus; whereas, only 33.33% of AR-Y764H protein underwent nuclear translocation, which was significantly lower than the AR-WT ($P < 0.05$) (Fig. 3e, f, p). At 1-nM DHT, 68.53% of AR-WT protein translocated into the nucleus. However, the nuclear translocation ratio of the mutant protein was only 45.35% (AR-WT vs. AR-Y764H, $P < 0.001$) (Fig. 3h, i, p). Surprisingly, when the DHT concentration increased to 10–100 nM, AR-WT almost completed nuclear translocation (81.77–92.20%), and AR-Y764H also completed considerable nuclear translocation (81.39–90.60%). Fluorescence signal was difficult to detect in the cytoplasm (AR-WT vs. AR-Y764H, no significance) (Fig. 3k, l, n–p).

Discussion

CAIS-affected individuals have female external genitalia and are generally raised as females. Their gonads are often detected in the inguinal canals, although they can be located anywhere from the abdomen to the scrotum. PAIS-affected individuals have variable clinical presentations ranging from almost normal masculinization to almost complete feminization (Mendoza and Motos 2013). In this study, we identified a same hemizygous mutation of Y764H in the *AR* gene in two siblings with CAIS and PAIS phenotypes. In vitro functional study showed that the cells with *AR*-Y764H mutation exhibited residual AR activity at high DHT concentrations. To our knowledge, this study is the first to demonstrate the functional consequence of the variant p.Y764H.

Although the p.Y764H (c.2290T > C) variant of the *AR* gene was reported to be a causative factor of CAIS by Quigley in 1995, no structural and functional studies of the

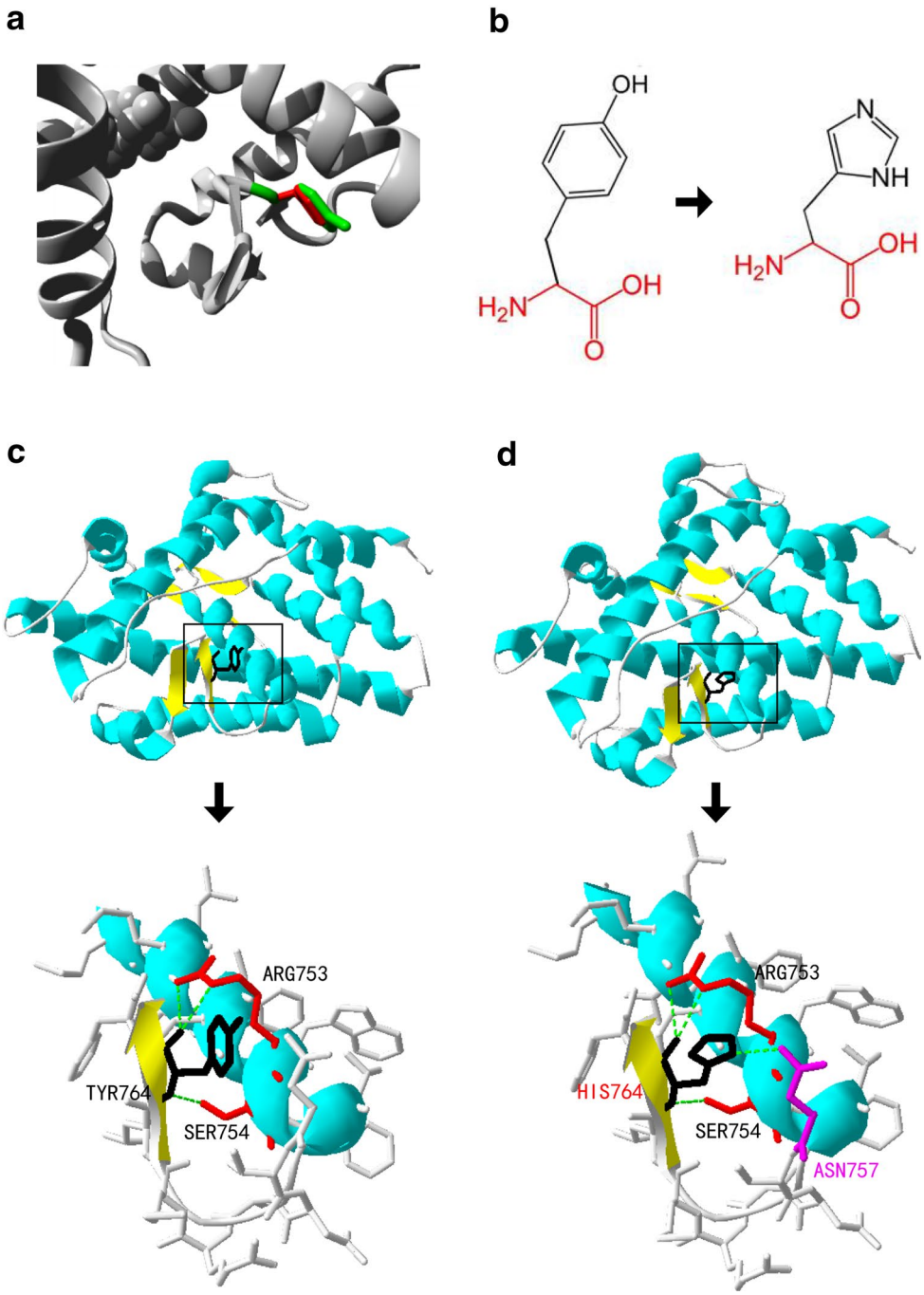

Fig. 2 Crystallographic modeling of AR protein. **a** The 3D-structure of AR protein provided by HOPE. The protein is colored gray, and the side chains of both the wild-type and the mutant residues are shown and colored green and red, respectively. **b** The figure shows the schematic structures of the original (left) and the mutant (right) amino acid. The backbone, the same for each amino acid, is colored red. The side chain, unique for each amino acid, is colored black. **c, d** Spatial conformation of both the wild-type and mutant residues of AR provided by SWISS PDB viewer. **c** The overall view of the protein structure of wild-type AR and the close-up view of codon 764. The rectangle-marked area was amplified and shown below. TYR764 (black) connected to ARG753 (red) with two hydrogen bonds (green), and linked to SER754 (red) with one hydrogen bond (green). The dotted line represents the hydrogen bond. **d** The overall view of the protein structure of mutant AR and the close-up view of the mutated site. TYR764 mutated to HIS764, and the connected hydrogen bonds and the spatial protein conformation were changed. Mutated residue HIS764 (black) still attached to ARG753 (red) with two hydrogen bonds (green) and SER754 (red) with one hydrogen bond (green) and also linked to ASN757 (purple) with another hydrogen bond (green). TYR: tyrosine; ARG: arginine; SER: serine; HIS: histidine; ASN: asparagine

mutation were undertaken and no patients with PAIS have since been reported with this mutation (Quigley and Bellis 1995). In this study, we identified the nonsynonymous Y764H hemizygous mutation not only in a patient with CAIS but also in a patient with PAIS from the same family. Other missense mutations at codon 764 have also been described earlier. The mutation p.Y764N (c.2290T > A) has been identified in a patient with CAIS by Yuan et al. (2018), while another mutation Y764C caused by an A > G substitution at site c.2291 was found in patients with PAIS, and predicted to affect DHT-induced receptor dimerization (McPhaul and Marcelli 1991; Murono and Mendonca 1995; Melo and Mendonca 2003; Nadal and Prekovic 2017). A nonsense mutation p.Y764X was also detected in a patient with CAIS (Cheikhelard and Morel 2008). These studies suggested that point mutations at codon 764 was likely to impair the function of AR protein resulting in AIS.

There were no other different pathogenic mutations in *AR* gene or other 46,XY DSD-related genes caused the difference between the two siblings in the study. Why the

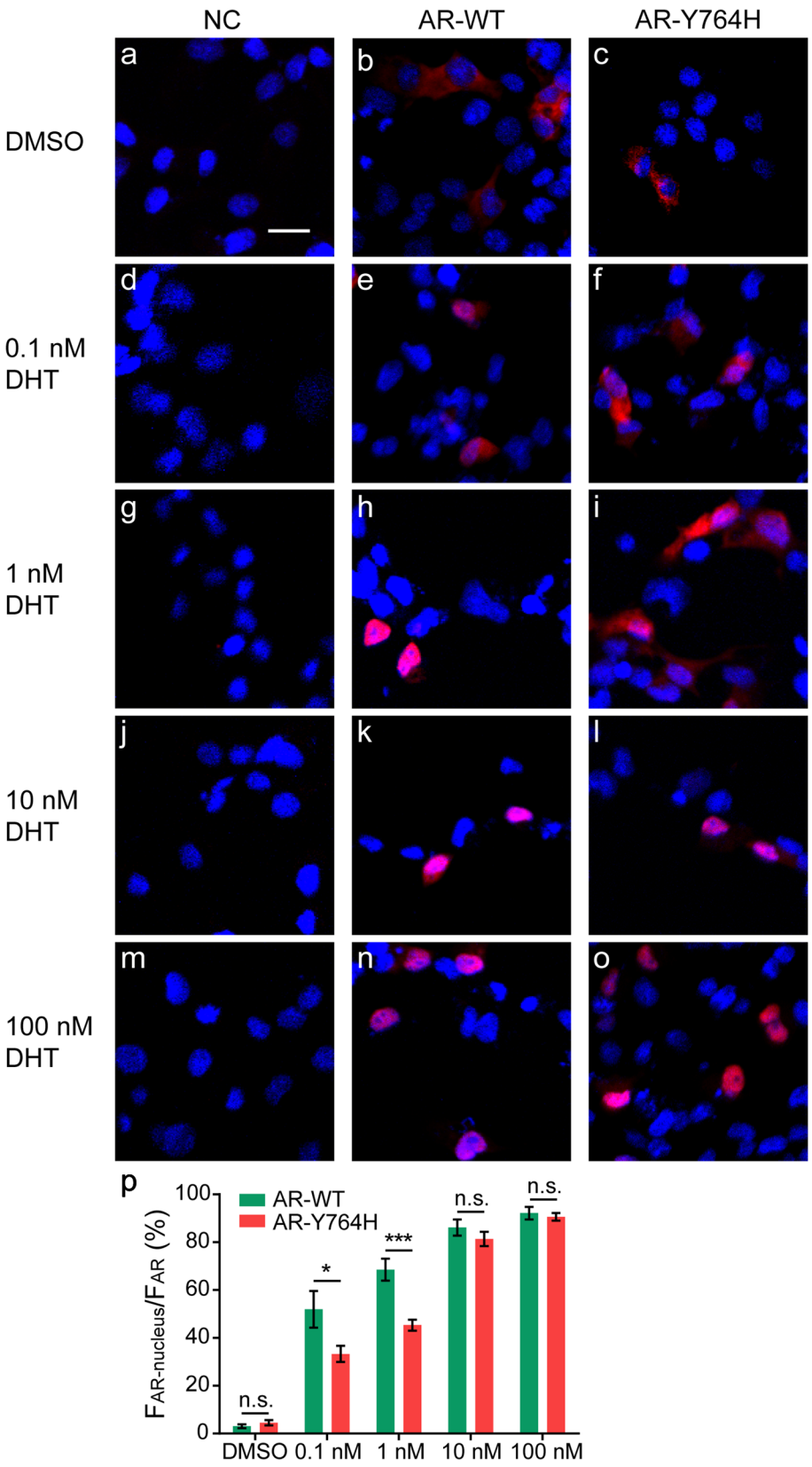

Fig. 3 Subcellular localization of wild-type and mutant AR proteins in COS-7 cells. COS-7 cells transiently transfected with *AR*-WT plasmid, *AR*-Y764H plasmid, or negative control plasmid (empty vector). Transfected cells were incubated with DMSO or DHT (0.1–100 nM) to assess the nuclear translocation of wild-type and mutant proteins. Cells transfected with an empty vector were used as a negative control. AR-WT and AR-Y764H fusions were stained with antibody (red) and measured for immunofluorescence. Nuclei were stained with DAPI (blue). Scale bar = 20 µm. *NC* negative control, *WT* wild type. **a, d, g, j, m** No red fluorescence was detected in COS-7 cells, which were transfected with empty vector and incubated with DMSO or DHT (0.1–100 nM). **b, e, h, k, n** The intracellular localization of AR-WT in COS-7 cells, which were incubated with DMSO or DHT (0.1–100 nM). **c, f, i, l, o** The intracellular localization of AR-Y764H in COS-7 cells, which were incubated with DMSO or DHT (0.1–100 nM). **p** Immunofluorescence quantitative analysis of AR-WT and AR-Y764H fusions in COS-7 cells. The X-axis represents different concentrations of DHT. $F_{\text{AR-nucleus}}$ represents the fluorescence intensity of AR protein in nucleus. F_{AR} represents the fluorescence intensity of AR protein in whole cells, including nucleus and cytoplasm. $F_{\text{AR-nucleus}}/F_{AR}$ indicated the nuclear translocation ratio of AR protein. *n.s.* no significance. $^{*}P < 0.05$, $^{***}P < 0.001$, Error bars represent the SEM

individuals sharing the same mutation exhibit different phenotypes? Several hypotheses exist: 1. the level of AR coactivators and corepressors; 2. the activity of 5α-reductase type 2; 3. the role of AR interacting proteins; 4. the presence of somatic mosaicism at a post zygote stage (Kohler and Lumbroso 2005; Kulshreshtha and Philibert 2009; Batista and Costa 2018). Our results showed that DHT concentration influences the extent of impairment of nuclear translocation in the Y764H variant. However, specific correlations between the Y764H mutation and different phenotypes of AIS need further investigation.

Structural analysis helps us to better understand the function of the mutant protein. The mutation is found in the β-strand S1 of the LBD region, which is arranged in a three-layered antiparallel α-helical sandwich fold with a hydrophobic cavity. The LBD region is essential for specific hormone-receptor binding, nuclear translocation, protein dimerization, and androgen-induced transcription (Matias and Donner 2000; Centenera and Harris 2008; Nadal and Prekovic 2017). TYR764 interacts with ARG753 and SER754 through hydrogen bonds, to stabilize the β-strand S1 (Nadal and Prekovic 2017; Paris and Boulahtouf 2018). The mutation of tyrosine to histidine at position 764 resulted in the loss of hydrophobic interactions and hydrogen bond changes in the mutant protein, thereby altering the stability and function of AR protein to some extent.

A recent study showed that the W752G mutation in *AR* led to the collapse of AR transactivation at whatever the androgen concentration was; whereas, the W752R mutation exhibited more than 50% of the wild-type AR transcriptional activity at high androgen concentration. The authors, therefore, emphasized the usefulness of in vitro studies to help direct the attention to pubertal virilization defect in patients with W752R mutation (Paris and Boulahtouf 2018). Our study showed the effect of *AR*-Y764H mutation on the function of the mutated protein by impairing its translocation from cytoplasm to the nucleus at lower DHT concentration. However, the mutated protein showed similar nuclear translocation ability as the wild type at higher androgen concentrations, which indicated that individuals with this mutation not abolished completely the function of AR protein.

In conclusion, we identified an *AR* gene variant Y764H that can cause different phenotypes in a family. To our knowledge, this study identified, for the first time, an *AR*-p.Y764H mutation in a patient with PAIS. Furthermore, we provide a strong evidence that the extent to which this variant impaired nuclear translocation is dependent on DHT concentrations. We hypothesize that the residual AR activity in PAIS could play a greater role at high DHT concentration which could be used to treat PAIS patients who were raised as males. Moreover, whether the AIS patients carrying *AR*-p.Y764H mutation raised as females exhibit virilization at puberty needs to be further studied by animal experiments and clinical researches. In addition, further studies in detail concerning the correlations between the variant and different phenotypes are needed. We believe the results of our study advance the understanding of further treatment of AIS.

Acknowledgements The project was financially supported by the Key Subject Program from Shanghai Municipal Commission of Health and Family Planning (2016ZB0102), Yangtze River Delta Project of Shanghai Science and Technology Commission (13495810300), Shanghai Collaborative Innovation Center for Translational Medicine (TM201611), Medical Professionals Cross Research Fund of Shanghai Jiao Tong University (YG2015MS39) and Jin Lei Pediatric Endocrinology Growth Research Fund for Young Physicians (PEGRF201506002). The funding organizations had no role in study design, data collection, and analysis, preparation of the manuscript, or in the decision to submit the article for publication.

Compliance with ethical standard

Conflict of interest The authors declare that they have no conflict of interest.

Ethics approval The research has been performed following the principles of the Declaration of Helsinki. In addition, the study was approved by the ethics committee of Shanghai Children's Hospital.

Informed consent Patients consented to participate in this study.

References

Bashamboo A, McElreavey K (2016) Mechanism of sex determination in humans: insights from disorders of sex development. Sex Dev 10(5–6):313–325. https://doi.org/10.1159/000452637

Batista RL, Costa EMF et al (2018) Androgen insensitivity syndrome: a review. Arch Endocrinol Metab 62(2):227–235. https://doi.org/10.20945/2359-3997000000031

Boehmer AL, Brinkmann O et al (2001) Genotype versus phenotype in families with androgen insensitivity syndrome. J Clin Endocrinol Metab 86(9):4151–4160. https://doi.org/10.1210/jcem.86.9.7825

Centenera MM, Harris JM et al (2008) The contribution of different androgen receptor domains to receptor dimerization and signaling. Mol Endocrinol 22(11):2373–2382. https://doi.org/10.1210/me.2008-0017

Chauhan P, Rani A et al (2018) Complete androgen insensitivity syndrome due to mutations in the dna-binding domain of the human androgen receptor gene. Sex Dev. https://doi.org/10.1159/000492261

Cheikhelard A, Morel Y et al (2008) Long-term followup and comparison between genotype and phenotype in 29 cases of complete androgen insensitivity syndrome. J Urol 180(4):1496–1501. https://doi.org/10.1016/j.juro.2008.06.045

Gottlieb B, Beitel LK et al (2012) The androgen receptor gene mutations database: 2012 update. Hum Mutat 33(5):887–894. https://doi.org/10.1002/humu.22046

Hughes IA, Davies JD et al (2012) Androgen insensitivity syndrome. Lancet 380(9851):1419–1428. https://doi.org/10.1016/S0140-6736(12)60071-3

Hughes IA, Werner R et al (2012) Androgen insensitivity syndrome. Semin Reprod Med 30(5):432–442. https://doi.org/10.1055/s-0032-1324728

Infante JB, Alvelos MI et al (2016) Complete androgen insensitivity syndrome caused by a novel splice donor site mutation and activation of a cryptic splice donor site in the androgen receptor gene. J Steroid Biochem Mol Biol 155(Pt A):63–66. https://doi.org/10.1016/j.jsbmb.2015.09.042

Jaaskelainen J (2012) Molecular biology of androgen insensitivity. Mol Cell Endocrinol 352(1–2):4–12. https://doi.org/10.1016/j.mce.2011.08.006

Kohler B, Lumbroso S et al (2005) Androgen insensitivity syndrome: somatic mosaicism of the androgen receptor in seven families and consequences for sex assignment and genetic counseling. J Clin Endocrinol Metab 90(1):106–111. https://doi.org/10.1210/jc.2004-0462

Kulshreshtha B, Philibert P et al (2009) Phenotype, hormonal profile and genotype of subjects with partial androgen insensitivity syndrome: report of a family with four adult males and one child with disorder of sexual differentiation. Andrologia 41(4):257–263. https://doi.org/10.1111/j.1439-0272.2009.00921.x

Matias PM, Donner P et al (2000) Structural evidence for ligand specificity in the binding domain of the human androgen receptor. Implications for pathogenic gene mutations. J Biol Chem 275(34):26164–26171. https://doi.org/10.1074/jbc.M004571200

McPhaul MJ, Marcelli M et al (1991) Molecular basis of androgen resistance in a family with a qualitative abnormality of the androgen receptor and responsive to high-dose androgen therapy. J Clin Investig 87(4):1413–1421. https://doi.org/10.1172/JCI115147

Melo KF, Mendonca BB et al (2003) Clinical, hormonal, behavioral, and genetic characteristics of androgen insensitivity syndrome in a Brazilian cohort: five novel mutations in the androgen receptor gene. J Clin Endocrinol Metab 88(7):3241–3250. https://doi.org/10.1210/jc.2002-021658

Mendoza N, Motos MA (2013) Androgen insensitivity syndrome. Gynecol Endocrinol 29(1):1–5. https://doi.org/10.3109/09513590.2012.705378

Murono K, Mendonca BB et al (1995) Human androgen insensitivity due to point mutations encoding amino acid substitutions in the androgen receptor steroid-binding domain. Hum Mutat 6(2):152–162. https://doi.org/10.1002/humu.1380060208

Nadal M, Prekovic S et al (2017) Structure of the homodimeric androgen receptor ligand-binding domain. Nature Commun 8:14388. https://doi.org/10.1038/ncomms14388

Nagaraja MR, Gubbala SP et al (2019) Molecular diagnostics of disorders of sexual development: an Indian survey and systems biology perspective. Syst Biol Reprod Med 65(2):105–120. https://doi.org/10.1080/19396368.2018.1549619

Paris F, Boulahtouf A et al (2018) Functional and structural study of the amino acid substitution in a novel familial androgen receptor mutation (W752G) responsible for complete androgen insensitivity syndrome. Sex Dev. https://doi.org/10.1159/000491114

Quigley CA, De Bellis A et al (1995) Androgen receptor defects: historical, clinical, and molecular perspectives. Endocr Rev 16(3):271–321. https://doi.org/10.1210/edrv-16-3-271

Sakkiah S, Ng HW et al (2016) Structures of androgen receptor bound with ligands: advancing understanding of biological functions and drug discovery. Expert Opin Ther Targ 20(10):1267–1282. https://doi.org/10.1080/14728222.2016.1192131

Vaidyanathan P, Kaplowitz P (2018) Partial androgen insensitivity syndrome presenting as pubertal gynecomastia: clinical and hormonal findings and a novel mutation in the androgen receptor gene. Endocrinol Diabetes Metab Case Rep. https://doi.org/10.1530/EDM-18-0128

Venselaar H, Beek TA et al (2010) Protein structure analysis of mutations causing inheritable diseases. An e-Science approach with life scientist friendly interfaces. BMC Bioinform 11:548. https://doi.org/10.1186/1471-2105-11-548

Wang Q, Lu J et al (2001) Ligand- and coactivator-mediated transactivation function (AF2) of the androgen receptor ligand-binding domain is inhibited by the cognate hinge region. J Biol Chem 276(10):7493–7499. https://doi.org/10.1074/jbc.M009916200

Yuan SM, Zhang YN et al (2018) Phenotypic and molecular characteristics of androgen insensitivity syndrome patients. Asian J Androl 20(5):473–478. https://doi.org/10.4103/aja.aja_17_18